Available online at www.sciencedirect.com
SCIENCE DIRECT®
Polymer 45 (2004) 865–872
polymer
www.elsevier.com/locate/polymer

Enhancement of color purity in blue-emitting fluorene–pyridine-based copolymers by controlling the chain rigidity and effective conjugation length

Wei Yang*, Jian Huang, Chuanzhen Liu, Yuhua Niu, Qiong Hou, Renqiang Yang, Yong Cao

Institute of Polymer Optoelectronic Materials and Devices, South China University of Technology, Wushan road, Guangzhou 510640, China

Received 9 March 2003; received in revised form 12 November 2003; accepted 27 November 2003

Abstract

A series of high molecular weight, readily soluble copolymers of 9,9-dioctylfluorene with pyridine (less than or equal to 50 mol%) are synthesized by Suzuki polycondensation. Copolymers emit blue light and exhibit high PL efficiency. PL efficiencies show the maximum at 3,5-pyridine content of around 30 mol% in the copolymer. With further the increase of *meta*-linkage contents, PL efficiencies decrease rapidly to15% for alternating copolymer. Cyclic voltammetry investigation reveals that LUMO levels of copolymers increase with the increase of pyridine content. The introduction of pyridine unit at 3,5-position into polyfluorene backbone significantly depresses the excimer formation. The intensity of excimer emission decreases with the increase of 3,5-pyridine contents. Narrow and pure blue EL emission is obtained for copolymer with pyridine content of 40 mol%. External quantum efficiency is moderately high (0.4–0.5%) for such a pure blue emitter. The threshold voltages of devices from copolymers with the pyridine content of less than 40 mol% are low in the range of 5–6 V based on the device configuration: ITO/PEDOT/polymer/Ba/Al. The results indicate that fluorene-*co*-3,5-pyridine copolymers are promising blue-emitting electroluminescent materials.

Keywords: Fluorene; Blue-emitting copolymer; Color purity

1. Introduction

Conjugated polymers have recently attracted great attention due to their possible utilization in flat panel displays [1]. Following the discovery of electroluminescence (EL) in poly(*p*-phenylenevinylene) (PPV) [2], various EL conjugated polymers have been synthesized [3–5]. Of them, blue-emitting polymers are still far away from specifications required by full color displays due to large band-gap, high oxidation potential and low electron affinities for blue EL polymers.

Poly(9-alkylfluorene)s are promising electroluminescent polymer for light-emitting diodes because of their thermal and chemical stability, good solubility in the common organic solvents, and high fluorescent quantum yields in the solid-state [6]. Poly(9,9-dioctylfluorene) (PDOF) exhibits very good, non-dispersive hole transport, but poor electron transport [7,8]. To achieve high quantum efficiency in a PDOF light-emitting diode, it is important to balance the electron and hole currents. Rigid-rod polyfluorene has a tendency toward a nematic type of packing arrangement in the bulk, and thus is inherently prone to chain aggregation that leads to a red-shifted emission [9] and to a reduction of emission efficiency [10]. Introduction of kink linkages to the polymer main chain is a widely accepted way to gain control of conjugated length and blue light emission [11,12]. Different kinds of disorder units are introduced to polyfluorene conjugated system, such as carbazole [13], end-capping [14], polyphenylene dendrimer substituents [15], distyrylbenzene [16], 5,7-dihydrodibenzo-oxepin and dibenzo-thiepine [17]. The resulted copolymers exhibit better spectral properties than fluorene homopolymer.

Polypyridine (PPy), with electron-accepting imine structure, is both luminescent and oxidative stable, thus attracting interest in potentially useful material in electronic and photonic devices. It has, for example, been employed with some success as an electron transport layer within

* Corresponding author. Tel.: +86-020-87112321; fax: +86-020-87114535.
E-mail address: pswyang@scut.edu.cn (W. Yang).

0032-3861/$ - see front matter © 2003 Elsevier Ltd. All rights reserved.
doi:10.1016/j.polymer.2003.11.052

polymer light-emitting diodes, affording improved device efficiencies [18]. Synthesis of alternating pyridine-based backbone copolymers with substituted phenylene [19,20] and fluorene units [21] have been reported for tunability of electronic properties with enhanced stability. Recently, Tammer and coworkers reported synthesis and characterization of random copolymers of '*para*' poly(2,5-pyridinediyl) and '*meta*' poly(2,6-pyridinediyl) and demonstrated possibility of control the chain rigidity and the effective conjugation length by the variation of the ratio of '*para*' to '*meta*' [22].

In this paper, the *meta* pyridine linkage, as the π-accepting moiety, has first been introduced into poly(2,7-(9,9-dioctyl)fluorene). We intend to introduce a 'kink' disorder on the conjugated main chain to depress the aggregation phenomenon and to enhance the color purity in blue-emitting polyfluorene. Different pyridine unit ratios in the polymer composition are incorporated to study the trend of the properties. The schematic illustration for this strategy is shown in Scheme 1.

2. Experiments

2.1. Instrumentation

^{1}H and ^{13}C NMR spectra were recorded on Bruker DRX-400 NMR Instrument in deuterated chloroform solution at 25 °C. The molecular weight of the polymers was determined by Waters GPC 2410 in THF via a calibration curve of polystyrene standards. Elemental analysis was performed on Vario EL Elemental Analysis Instrument (Elementar Co.). Thermogravimetric analysis(TGA) measurements were performed on Netzsch TG 209 under N_2 at a heating rate of 20 °C/min. Differential scanning calorimetry (DSC) measurements were performed on Netzsch DSC 204 under N_2 at a heating rate of 10 °C/min. Cyclic voltammetry (CV) was recorded on a computer-controlled CHI660A electrochemical workstation. A glass–carbon electrode (~0.1 cm^2) was coated with a thin film from chloroform solution of polymers and used as the working electrode. A platinum wire was used as the counter electrode and an Ag/AgCl electrode used as the reference electrode at a scan rate of 50 mV/s in a nitrogen-saturated solution of 0.1 M tetrabutylammonium hexafluorophosphate (Bu_4NPF_6) in acetonitrile (CH_3CN). UV–vis absorption spectra were recorded on a HP 8453 spectrometer. PL quantum yields were determined in integrating sphere IS080 with 325 nm excitation of He–Cd laser (Mells Griod) or with 405 nm of solid state laser (Crystal Laser). EL efficiencies were achieved with calibrated silicon photodiode. PL and EL spectra were recorded by using Instaspec 4 CCD spectrophotometer (Oriel Co.).

The surface morphology was investigated using tapping-mode atomic force microscopy (AFM) (Thermo. Auto Probe C P Res.). AFM images of the films (100-nm-thick layer) spun from a toluene solution of polymers at 2000 rpm on indium tin oxide (ITO) substrates coated with a 30-nm-thick layer of poly (ethylene dioxythiophene) doped with polystyrene sulfonic acid (PEDOT:PSS).

2.2. Materials

Fluorene, *n*-butyllithium, *n*-octylbromide, 2-isopropoxy-4,4,5,5-tetramethyl-1,3,2-dioxaborolane, 3,5-dibromopyridine and tetraethylammonium hydroxide were purchased from Aldrich Co. Tetrakis(triphenylphosphine) palladium was obtained from TCI Co. Anhydrous tetrahydrofuran was distilled over sodium/benzophenone under nitrogen prior to use. Chloroform and toluene were distilled over calcium chloride. 9,9-Dioctylfluorene (1) and 2,7-dibromo-9,9-dioctylfluorene (2) were prepared according to the published procedures [23]. 2,7-Bis(4,4,5,5-tetramethyl-1,3,2-dioxaborolan-2-yl)-9,9-dioctylfluorene (3) [21]. *n*-Butyllithium (19.7 ml of a 1.6 M solution in hexane, 31.45 mmol) was dropwise added into a solution of 2,7-dibromo-9,9-dioctylfluorene (2) (5.6 g, 10.22 mmol) in THF (130 ml) at −78 °C. The mixture was stirred at

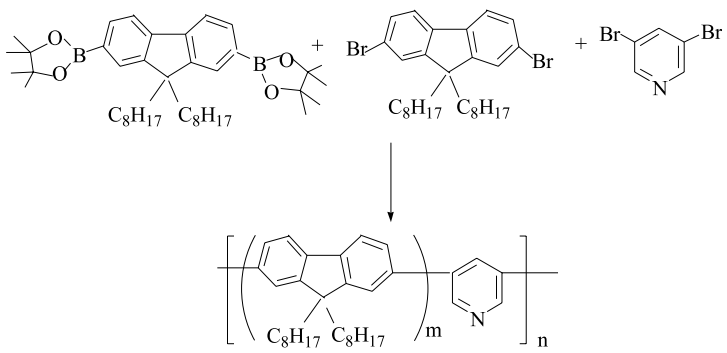

Comonomer ratio: 90/10 (PFPy 10), 80/20 (PFPy 20),

70/30 (PFPy 30), 60/40(PFPy 40), 50/50(PFPy 50)

Scheme 1. Synthesis route of the copolymers.

−78 °C for 2 h, 2-isopropoxy-4,4,5,5-tetramethyl-1,3,2-dioxaborolane (25 ml, 123.24 mmol) was added rapidly to the solution, and the mixture was stirred at −78 °C for 2 h. Then the mixture was warmed up to a room temperature and stirred for another 36 h. The mixture was poured into water and was extracted with ether. The organic layer was washed with brine and dried over an anhydrous magnesium sulfate. The solvent was removed under a reduced pressure. The crude product was purified by column chromatography (silical gel, 10% ethyl acetate in hexane) to make the product shown in the title as a white solid, (Mp = 128–131 °C) in 46% yield. ^{1}H NMR (500 MHz, $CDCl_3$, ppm): 7.81 (d, 2H), 7.74 (s, 2H), 7.71 (d, 2H), 1.99 (m, 4H), 1.39 (s, 24H), 1.22–1.00 (m, 20H), 0.81 (t, 6H), 0.56 (m, 4H); ^{13}C NMR (100 MHz, $CDCl_3$, ppm): 150.86, 144.30, 134.04, 129.29, 119.77, 84.11, 55.57, 40.49, 32.18, 30.33, 29.58, 25.33, 23.98, 22.99, 14.48. Element Anal. Calcd for $C_{41}H_{64}O_4B_2$: C, 76.74%, H, 10.04%. Found: C, 76.44%; H, 9.90%.

2.3. Polymer synthesis [24]

Carefully purified 2,7-dibromo-9,9-dioctylfluorene, 2,7-bis(4,4,5,5-tetramethyl-1,3,2-dioxaborolan-2-yl)-9,9-dioctylfluorene, 3,5-dibromo-pyridine and $(PPh_3)_4Pd(0)$ (0.5–1.5 mol%) were dissolved in a mixture of toluene and $(C_2H_5)_4NOH$ (20%) aqueous solution. Under argon atmosphere the solution was refluxed by vigorous stirring for 48 h. The whole mixture was poured into methanol. The precipitated material was recovered by filtration through a funnel and washed with acetone to remove oligomers and catalyst residues. Seven copolymers with different compositions were synthesized from various starting molar ratios of DOF to Py: 99:1, 95:5, 90:10, 80:20, 70:30, 60:40 and 50:50. The isolated copolymers were obtained in 70–80% yield. The resulted polymers were soluble in common organic solvents (chloroform or tetrahydrofuran). ^{1}H NMR (500 MHz, $CDCl_3$, ppm): with PFPy50: 8.29 (2H), 8.26 (1H), 7.95 (2H), 7.90 (2H), 7.84 (2H), 2.22 (4H),1.14 (24H) and 0.79 (6H); ^{13}C NMR (100 MHz, $CDCl_3$, ppm): 156.92, 152.29, 142.15, 138.76, 137.85, 126.54, 121.83, 120.66, 118.96, 55.80, 41.02, 32.24, 30.62, 29.74, 24.36, 22.94 and 14.38. The results of elemental analyses of nitrogen and carbon for each copolymer were used for calculation of actual copolymer composition. Element Anal. Found: for PFPy5: C, 88.74%; N, 0.21%; for PFPy10: C, 82.25%; N,0.30%; for PFPy20: C, 88.56%; N, 0.59%; for PFPy30: C, 88.32%; N, 1.07%; for PFPy50: C, 86.92%; N, 2.78%.

3. Results and discussion

3.1. Synthesis and characterization of copolymers

Various high molecular weight, readily soluble copolymers from 2,7-dibromo-9,9-dioctylfluorene, 2,7-bis(4,4,5,5-tetramethyl-1,3,2-dioxaborolan-2-yl)-9,9-dioctylfluorene and comonomer 3,5-dibromo-pyridine were prepared by using palladium catalyzed Suzuki polycondensation (Scheme 1). The comonomer feed ratios of DOF to Py are 99:1, 95:5, 90:10, 80:20, 70:30, 60:40 and 50:50 and the corresponding copolymers are named PFPy1, PFPy5, PFPy10, PFPy20, PFPy30, PFPy40 and PFPy50, respectively. The starting monomer ratios have been adjusted in order to investigate the effect of copolymer composition on the physical and optical properties. The actual ratio of DOF to Py in the copolymer calculated from elemental analysis is close to the feed ratio as listed in Table 1. When the concentration of Py in the copolymers is less than 50 mol%, the resulted polymers are kinds of special random copolymers that consist of the fluorene segment of different lengths separated by a single pyridine unit from both sides of each segment. When the concentration of pyridine is equal to 50 mol%, the copolymer has a regular alternating A–B structure. Copolymers obtained are of relatively high molecular weight with a polydispersity index (M_w/M_n) from 1.2 to 2.5 (Table 1). The random copolymers have higher molecular weights than the alternating copolymer.

The thermal properties of polymers are evaluated by TGA and DSC measurement. TGA reveals excellent thermal stabilities of homo- and co-polymers under nitrogen. As shown in Table 1, the decomposition temperature (5% weight loss) is 385 °C for homopolymer and about 400 °C for copolymers. Thermally induced phase transition behavior of polymers is investigated by DSC. The glass transition temperatures (T_g) of polymers slightly rise from 70 to 93 °C with the increase of Py content. This indicates that the interchain interaction increases in the copolymers. The phase transition temperature from partially crystalline state to liquid crystalline (T_{Cr-LC}) of PDOF is 155 °C. The T_{Cr-LC} values of copolymers are much less than that of homopolymer (Table 1), due to the decrease of chain regularity by the *meta*-linkage along the polymer backbone.

3.2. Optical properties

The optical characteristics of polymers are investigated both in solution and in solid state. The absorption and emission spectral data for polymers are summarized in Table 2. UV–vis absorption spectra in diluted $CHCl_3$ solution of copolymers are depicted in Fig. 1(a). The spectra reveal a general trend of slightly increased blue-shift of λ_{max} with the increase of *meta*-pyridine content. The blue-shift is consistent with the reduction in π-conjugation induced by the introduction of the 3,5-pyridinediyl moieties. For fluorene homopolymer in thin film, the absorption spectrum is consistent with that reported previously [25]. Absorption profile is featured with a main peak at ca. 380 nm and a small sharp shoulder at 430 nm (Fig. 1(b)), the latter is interpreted as an evidence of β-phase formation in the glass phase of PDOF [18]. This interpretation is supported by the fact that 430 nm feature disappears in the solution spectrum

Table 1
Structural and thermal properties of polymers

Polymer	M_w ($\times 10^3$)	M_w/M_n	DOF/Py in feed composition	DOF/Py in copolymer	T_g (°C)	T_{lc} (°C)	TGA (5% loss) (°C)
PDOF	55.2	2.3	–	–	72	156	385
PFPy5	41.2	2.0	95/5	95/5	70	105	389
PFPy10	36.1	1.9	90/10	92/8	82	94	395
PFPy20	62.3	2.6	80/20	85/15	80	98	397
PFPy30	27.3	2.2	70/30	76/24	83	94	406
PFPy40	34.2	1.5	60/40	–	–	–	–
PFPy50	20.3	1.3	50/50	52/48	93	116	398

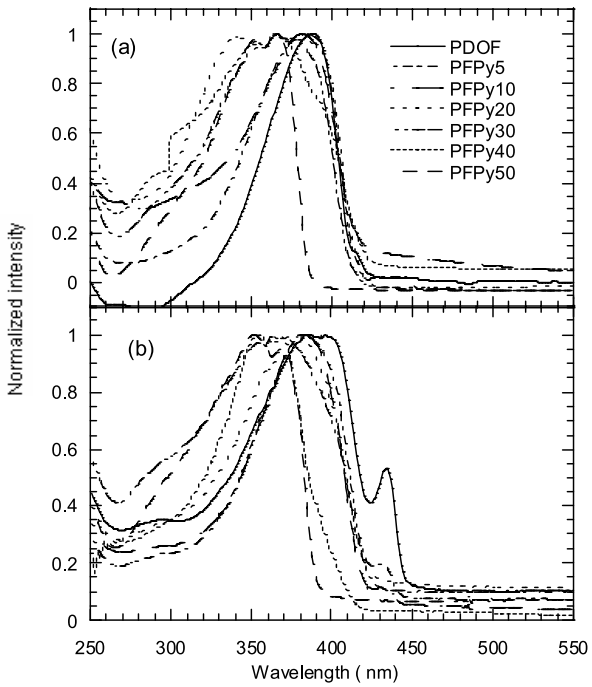

Fig. 1. (a) UV–vis absorption spectra for copolymers from in chloroform solution (10^{-4} mol/L) (b) UV–vis absorption spectra for copolymers from the spin-coated films on quartz plate.

(Fig. 1(a)). It is important to note that the intensity of 430 nm peak decreases substantially with incorporation of 5–10 mol% pyridine unit into polyfluorene backbone (Fig. 1(b)). This peak completely disappears once the pyridine content increases to ca. 20 mol% in the copolymers, which indicates that the incorporation of 3,5-linkage pyridine unit into polyfluorene chain really introduces the disorder in polymer backbone, as a result of which β-phase formation becomes impossible in the glass phase [26].

The optical band gaps (E_g) of polymers are 2.76–3.15 eV from the onset in the film absorption spectra. The absorption wavelengths of copolymers are blue-shifted with the increase of pyridine concentration. Among them the alternating copolymer shows the largest blue-shift ($\Delta\lambda = 40$ nm) in absorption spectra and the greatest increase in E_g (Table 2). The observed blue-shift suggests that the 3,5-pyridinediyl effectively decreases the conjugation length of polymer backbone, since the linear π-system is interrupted [27].

Photoluminescent (PL) spectra of copolymers shown in Fig. 2 reveal a similar trend, PL peaks being slightly blue-shifted with increasing the pyridine contents for random copolymers. In consistence with the absorption spectra, the alternating copolymer shows the largest blue-shift compared with others. The observed blue-shift in PL spectra is a further evidence of the reduced conjugation along the polymer backbone. PL efficiencies of copolymer films are listed in Table 2. The PL efficiency shows the maximum at pyridine content of around 30 mol% in the copolymers. With further increase of *meta*-linkage contents, the PL efficiency decreases rapidly to 15% for alternating copolymer. Such PL efficiency dependence is reproducible during repeating measurements. It is no clear that the origin of such complicated behavior of PL efficiencies vs. 3,5-pyridine contents. We note that similar transition point at around

Table 2
Optical properties of the copolymers

Polymer	λ_{max} (solution) Abs.[a] (nm)	λ_{max} (film) Abs. (nm)	Band gap E_g (eV)[b]	λ_{max} (solution) PL[a] (nm)	λ_{max} (film) PL (nm)	PL (%)
PDOF	386	391	2.76	443	422	47
PFPy5	380	380	2.79	420	422	30
PFPy10	385	383	2.79	420	422	28
PFPy20	361	380	2.90	418	420	51[c]
PFPy30	363	370	2.90	420	420	60[c]
PFPy40	362	380	2.97	418	419	49[c]
PFPy50	340	350	3.15	403	413	15[c]

[a] Data in solution (chloroform, 10^{-4} mol/L).
[b] Optical band gap derived from film absorption spectra.
[c] PL efficiencies of the polymers obtained with 325 nm excitation, the others with 405 nm.

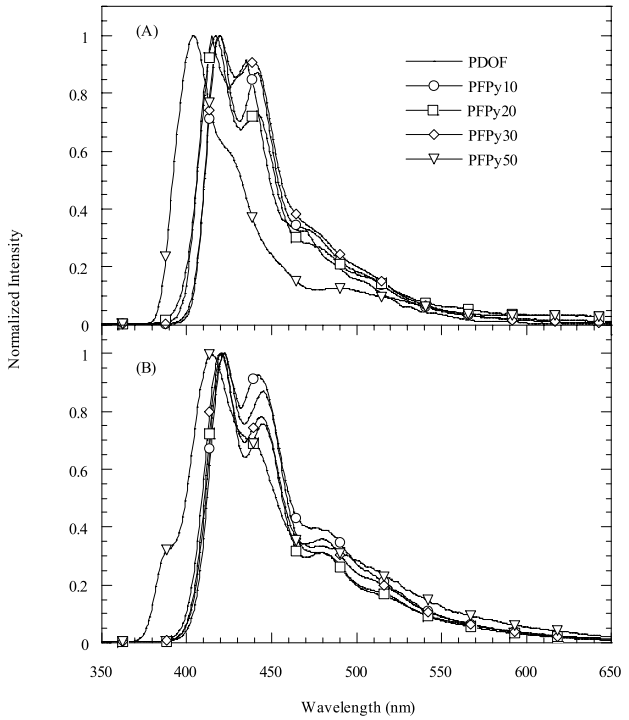

Fig. 2. (A) PL spectra for copolymers in chloroform solution (10^{-4} mol/L) (B) PL spectra for copolymers from the spin-coated films on quartz plate.

35% was reported by Tammer et al. [22] for random copolymers of '*para*' poly(2,5-pyrinediyl) and '*meta*' poly(2,6-pyrinediyl) (PPY-PmPY).They observed that PL emission peaks for copolymers with *meta*-linkage in composition between 0–35% are almost constant, peaked at around 535 nm as for '*para*' PPY homopolymer, while significantly blue-shifted with further increase of '*meta*' contents. They explained the observed phenomena by that at levels below 35%, the *meta* links gradually lose the chain rigidity, but at high levels (>35%) of the *meta* links reduce the effective conjugation length of the copolymers.

3.3. Electrochemical properties

The redox behavior of polymers is investigated by CV. As shown by the cyclic voltammograms in Fig. 3, the polymers exhibit partial reversibility in both n-doping and p-doping processes. The oxidation and reduction potentials derived from the onset of the electrochemical p-doping and n-doping are summarized in Table 3. HOMO and LUMO levels are calculated according to an empirical formula ($E_{HOMO} = -e(E_{ox} + 4.4)$ (eV) and $E_{LUMO} = -e(E_{red} + 4.4)$ (eV)) [28]. As shown in Table 2, HOMO and LUMO levels of the fluorene homopolymer are 5.77 and 2.16 eV, respectively. With the increase of pyridine contents, the oxidation potentials are almost unchanged up to the pyridine content of 40 mol% and the reduction potentials increase slightly. However, the alternating copolymer exhibits both the lower oxidation potential (by 0.41 V) and the higher reduction potential (by 0.17 V) compared with fluorene homopolymer. Moderate increase of LUMO levels of copolymers with increasing pyridine contents can be attributed to the increase of electron-withdrawing pyridinyl moieties in polymer backbone. We could expect the improvement in electron injection from the cathode in comparison with fluorene homopolymer.

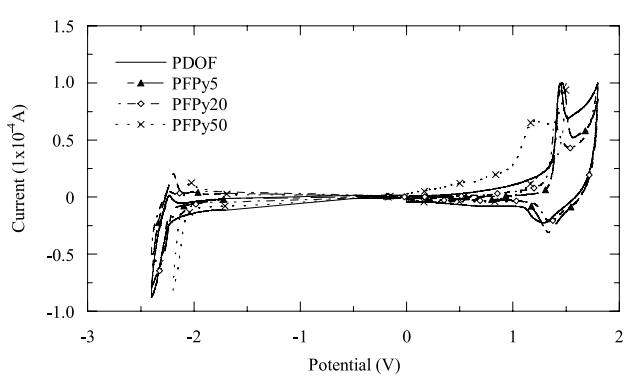

Fig. 3. Cyclic voltammograms of copolymers in 0.1 M. Bu_4NPF_6/CH_3CN solution at a scan rate of 50 mV/s.

From Table 3, it can be seen that the energy gaps (E'_g) between E (oxidation) and E (reduction), which are determined by CV, decrease as the pyridine contents of copolymers increase although the optical band-gaps increase (Table 2). This differences may be caused by the interface barriers between the polymer films and the electrode surfaces [29]. The electrochemical datum may be the combination of the optical band-gap and the interface barrier for charge injection that makes it larger [30]. Seki et al. [31] and Park et al. [32] investigated the interfaces between metals (Ca, Al) and organic emitting layers (PPV oligomer, Alq_3) and found the existence of an electric dipole layer at the interface and defined the potential differences between the outermost electrode surface and the first polymer layer as Δ. The formation of the interfacial dipole layer can modify the barrier height by the value of Δ. The general tendency of the direction and magnitude of Δ gives a guide line for applying the traditional method to the estimation of the barrier heights [31]. As for this system, there should be a hydrogen bond interaction between pyridine group and Si–O–H hydrogen atom on the surface of the glass–carbon electrode. Thus, N-containing polymer chains can be aligned in parallel with the surface of a

Table 3
Oxidation (E_{ox}) and reduction potential (E_{red}) of polymers

Polymer	E_{ox} (V)	E_{red} (V)	HOMO (eV)	LUMO (eV)	Energy gap E'_g (eV)
PDOF	1.37	−2.24	−5.77	−2.16	3.61
PFPy5	1.37	−2.21	−5.77	−2.19	3.58
PFPy10	1.35	−2.21	−5.75	−2.19	3.56
PFPy20	1.33	−2.18	−5.73	−2.22	3.51
PFPy30	1.34	−2.14	−5.74	−2.26	3.48
PFPy40	1.32	−2.13	−5.72	−2.27	3.45
PFPy50	0.96	−2.07	−5.36	−2.33	3.03

glass–carbon electrode [33]. In opposition to the optical band-gap, therefore, the barrier height might decrease with the increases of pyridine contents. As the effects of pyridine contents on the barrier height—both the direction and magnitude—overwhelm that on the optical band-gap, E_g's decrease with the increase of pyridine contents.

3.4. Electroluminescent properties

Fig. 4 shows the EL spectra of the homo-polymer and copolymers. Device configuration is as follows: ITO/PEDOT:PSS/polymer/Ba/Al. PEDOT is used as an anode buffer, and Ba is used as a cathode. As shown in Fig. 4, the intensity of excimer emission in visible region decreases with the increase of pyridine contents. Pure and narrow emission appears for the copolymer with 40 mol% pyridine content. As expected, a significant excimer emission appears for the alternating copolymer due to the high regularity of polymer chain. The results indicate that the introduction of *meta*-linkage pyridine in a certain comonomer ratio into polyfluorene backbone is effective in depression of excimer emission from Table 4. Except the alternating copolymer, the EL external quantum efficiencies of copolymers are very close, despite the fact that LUMO levels of copolymers increase with the increase of pyridine contents. The alternating copolymer shows a significant lower efficiency despite the observable decrease in its HOMO level (Table 3). These facts indicate that the device performances are controlled by carrier mobility rather than by electron and hole injection. Further evidence for this argument can be obtained from Table 5, where we compare device performances with the different anode buffers and cathodes. As can be seen from Table 5, no substantial improvements in device efficiencies are observed when PEDOT-PSS with work function of 5.0 eV [34] is replaced by PVK with work function of 5.8 eV [35,36], which matches HOMO level of PFPy copolymers (Table 3). Quantum efficiency could be evidently improved by replacing PEDOT-PSS with PVK buffer layer if the device efficiency is hole-injection limited. On the other hand, since device efficiencies are not improved with the increases of LUMO levels, the device efficiencies for such copolymers

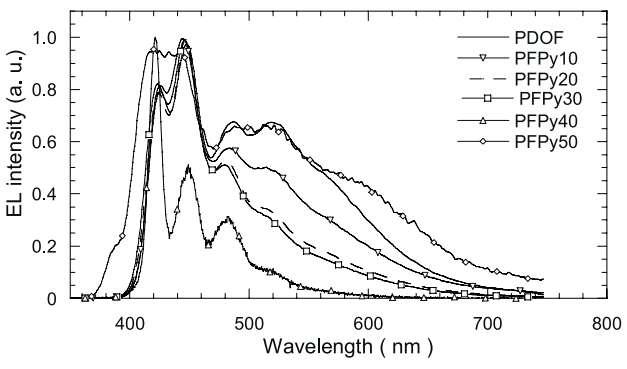

Fig. 4. EL spectra for the polymers.

Table 4
EL properties of the polymers

Polymer	Bias (V)	Current (mA)	Luminance (cd/m^2)	EQ (%)	EL_{max} (nm)	CIE coordinate X, Y
PDOF	4.8	24.9	501	0.52	456	0.20,0.20
PFPy 5	7.2	78.5	498	0.16	446	–,–
PFPy10	7.4	18.5	161	0.22	442	0.19,0.16
PFPy20	7.2	40.1	585	0.40	442	0.17,0.12
PFPy30	6.1	30.0	462	0.40	438	0.17,0.11
PFPy40	7.4	22.9	298	0.45	440	0.15,0.08
PFPy50	15.0	18.4	11	0.02	424	0.21,0.20

seem to be limited by low carrier mobility, which is the result of breaking π-conjugation by the introduction of *meta*-linkage of pyridine sites. Direct measurement of carrier (electron or hole) mobility for copolymers with different pyridine contents can provide the better understanding of structure-property relations in this interesting system.

Since film morphology is also important for device performances, the film surfaces are inspected by AFM. Fig. 5 illustrates AFM studies of the surfaces of fluorene homopolymer (a) and copolymer films (b, c) on ITO substrates. The copolymer films show the fine-scale phase separation in the range of 5–10 nm and have a root-mean-square (rms) roughness of about 0.5 nm. In contrast, the homopolymer exhibits large-scale phase separation in the diameter of 30–40 nm and has a rms roughness of 1.4 nm. Based on above results, the device performances could be further explained. Jakubiak et al. [37] reported that the aggregation of polymer chains enhances the excimer formation, which reduces the PL quantium efficiency. The films spun from different solvents also show different PL spectra. This observation suggests that the morphology of polymer has a remarkable effect on its emission spectrum [38]. The aggregate formation is found to be morphology dependent. The film from a good solvent leads to better interchain registry than from a poor solvent [39]. Toluene is a better solvent for homopolymer than for copolymers. We therefore, suggest the following origin for the morphology dependence of aggregation: homopolymer film from toluene in which the polymer is much better soluble, leading to a

Table 5
Device performances of copolymers using different cathodes and hole transfer layers

Device	Bias (V)	Current (mA)	Luminance (cd/cm^2)	Efficiency (%)
PEDOT/PFPy20/Ba/Al	7.2	40.1	585	0.40
PEDOT/PFPy20/Li/Al	8.8	5.5	94	0.27
PVK/PFPy20/Li/Al	19.2	5.0	73	0.15
PEDOT/PFPy1/Li/Al	9.8	11.4	250	0.35
PVK/PFPy1/Li/Al	14.5	4.5	63	0.22
PEDOT/PFPy20/LiF/Al	10.5	40.1	50	0.20
PVK/PFPy20/LiF/Al	16.2	3.0	15	0.08

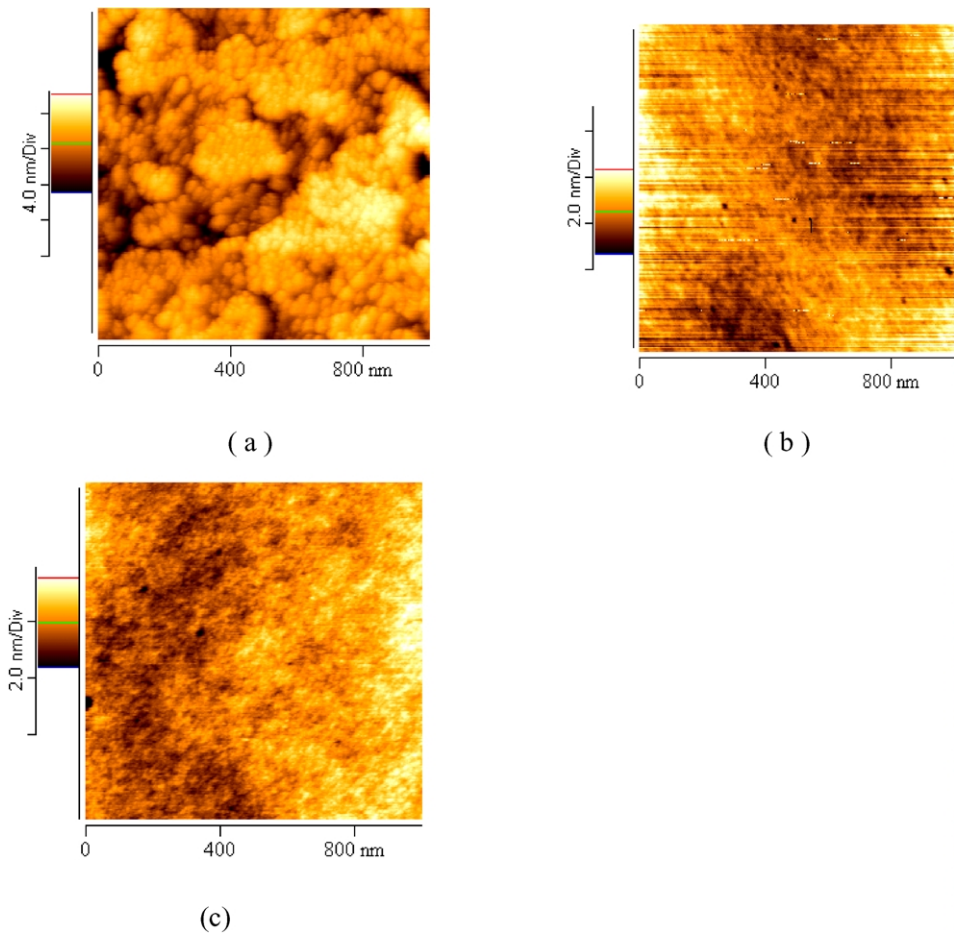

Fig. 5. Tapping-mode AFM topographic images of thin films spin-coated on ITO substrates from toluene solution of PDOF (a), PFPy40 (b) and PFPy50 (c).

more planar and extended conformation [40]. As a result, homopolymer forms a big aggregation (Fig. 5(a)). On the other hand, copolymers are less soluble in toluene, leading to a disordered coil-like conformation, and form a small aggregation [41] (Fig. 5(b) and (c)). The formation of aggregates is apparently detrimental to PL efficiency and leads to the red-shifted film spectra. That could explain why the device of homopolymer has an apparent red-shift emission as well as the device of copolymer (PFPy40) has a pure emission spectrum and a moderately high emission efficiency. As to the alternating copolymer, the apparent red-shift emission can't be explained only from the AFM morphological point of view. Considering there are large differences in molecular weight as well as in polydispersity index between homopolymer and copolymers, corresponding studies in this direction are in progress.

4. Conclusions

High molecular weight, readily soluble copolymers of 9,9-dioctylfluorene with pyridine (less than or equal to 50 mol%) are synthesized by Suzuki polycondensation. The introduction of pyridine unit at 3,5-position into polyfluorene backbone significantly depresses the excimer formation. The intensity of excimer emission decreases with the increases of pyridine contents. Narrow and pure blue EL emission is obtained for copolymer with the pyridine content of 40 mol%. External quantum efficiency is moderately high (0.4–0.5%) for such pure blue emitter. Device efficiency seems to be limited by low carrier mobility, which is the result of breaking π-conjugation by introduction of *meta*-linkage of pyridine sites.

Acknowledgements

This work is supported by MOST (Project No. 2002CB6613402), the National Natural Science Foundation of China (No. 50173008) and the Natural Science Foundation of Guang-dong Province (No. 011545).

References

[1] Gustafsson G, Cao Y, Treacy GM, Klavertter F, Colaneri N, Heeger AJ. Nature 1992;357:477.
[2] Burroughes JH, Bradly DDC, Brown AR, Marks RN, Markay K, Friend RH, Burns B, Holmes AB. Nature 1990;347:539.

[3] Grem G, Ledizky G, Ullrich B, Leising G. Adv Mater 1992;4:36.
[4] Yang Y, Pei Q, Heeger AJ. J Appl Phys 1996;79:934.
[5] Berggren M, Inganas O, Gustafsson G, Andersson MR, Hjertberg T, Wennerstrom O. Nature 1994;372:444.
[6] Klärner G, Lee J-I, Davey MH, Miller RD. Adv Mater 1999;11:115.
[7] Redecker M, Bradly DDC, Inbasekaran M, Woo EP. Appl Phys Lett 1998;73:1565.
[8] Campbell AJ, Bradly DDC, Antoniadis H. J Appl Phys 2001;89:3343.
[9] Bliznyuk VN, Carter SA, Scott JC, Klarner G, Miller RD, Miller DC. Macromolecules 1999;32:361.
[10] Bradley DDC, Grell M, Grice A, Tajbakhsh A, O'Brien D, Bleyer A. Opt Mater 1998;9:1.
[11] Ahn T, Jang MS, Shim H-K, Hwang DH, Zyung T. Macromolecules 1999;32:3279.
[12] Zheng M, Sarker AM, Gurel EE, Lahti PM, Karasz FE. Macromolecules 2000;33:7426.
[13] Xia C, Rigoberto CA. Macromolecules 2001;34:5854.
[14] Miteva T, Meisel A, Knoll W, Nothofer HG, Scherf U, Muller DC, Meerholz K, Yasuda A, Neher D. Adv Mater 2001;13(8):565.
[15] Setayesh S, Grimsdale AC, Weil T, Enkelmann V, Mullen K, Meghdadi F, List EJW, Leising G. J Am Chem Soc 2001;123:946.
[16] Holmes AB, Sano T, Fischmeister C, Frey J, Hennecke U, Tuan C, Chuah BS, Ma Y, Martin R, Rees ID, Li J, Bond AD, Cacialli F, Friend RH. Proc SPIE 2002;42:4464.
[17] Lim SF, Rees ID, Cacialli F, Holmes AB, Friend RH. ICSM-2002, China, Book Abstr 2002;229.
[18] Dailey S, Halim M, Rebourt E, Samuel IDW, Monkman AP. SPIE Proc 1997;82:3148.
[19] Tanaka S, Kumei M. Synth Met 1999;102:1524.
[20] Ng S-C, Lu H-F, Chan H-S-O, Fujii A, Laga T, Yoshino K. Adv Mater 2000;12(15):1122.
[21] Liu B, Yu W-L, Lai Y-H, Huang W. Chem Mater 2001;13:1984.
[22] Tammer M, Horsburgh L, Monkman AP, Brown W, Burrows HD. Adv Funct Mater 2002;12(6 and 7):447.
[23] Ranger M, Rondeu D, Leclerc ML. Macromolecules 1997;30:7686.
[24] Towns C, O'Dell R. WO 00/53656; 1999.
[25] Scherf U, List EJW. Adv Mater 2002;14(7):477.
[26] Grell M, Bradly DDC, Inbasekaran M, Ungar G, Whitehead KS, Woo EP. Synth Met 2000;111:579.
[27] Kleaner G, Miller RD. Macromolecules 1998;31:2007.
[28] Bredas JL, Silbey R, Boudreaux DS, Chance RR. J Am Chem Soc 1983;105:6555.
[29] Janietz S, Bradley DDC, Grell M, Giebeler C, Inbasekaran M, Woo EP. Appl Phys Lett 1998;73(17):2453.
[30] Chen ZK, Huang W, Wang L-H, Kang ET, Chen BJ, Lee CS, Lee ST. Macromolecules 2000;33:9015.
[31] Ishii H, Sugiyama K, Yoshimura D, Ito E, Ouchi Y, Seki K. IEEE J Sel Top Quantum Electron 1998;4:24.
[32] Park Y, Choong V, Ettendgui E, Gao Y, Hsieh BR, Wehrmeister T, Mullen K. Appl Phys Lett 1996;69:1080.
[33] Yamamoto T. Macromol Rapid Commun 2002;23:583.
[34] Cao Y, Yu G, Zhang C, Menon R, Heeger AJ. Synth Met 1997;87:171.
[35] Kido J, Hongawa K, Okuyama K, Nagai K. Appl Phys Lett 1994;64:815.
[36] Layla B, Francois TV, Olivier S. Synth Met 2001;122:351.
[37] Jakubiak R, Collion CJ, Wan WC, Rothberg LJ, Hsieh BR. J Phys Chem B 1999;103:2394.
[38] Blatchford JW, Gustafson TL, Epstein AJ, Vanden Bout DA, Kerimo J, Higgins DA, Barbarar PF, Fu D-K, Swager TM, MacDiarmind AG. Phys Rev B 1996;54(6):3683.
[39] Diaz-Garcia MA, Hide F, Schwartz BJ, Andersson MR, Pei Q, Heeger AJ. Synth Met 1997;84:455.
[40] Shi Y, Liu J, Yang YJ. Appl Phys 2000;87(9):4254.
[41] Blatchford JW, Jessen SW, Lin L-B, Gustafson TL, Fu D-K, Wang H-L, Swager TM, MacDiarmind AG, Epstein AJ. Phys Rev B 1996;54(13):9180.